HHS Public Access

Author manuscript

Immunohorizons. Author manuscript; available in PMC 2021 October 08.

Published in final edited form as:

Immunohorizons. ; 4(6): 352–362. doi:10.4049/immunohorizons.2000043.

Reduced Sialylation and Bioactivity of the Antifibrotic Protein Serum Amyloid P in the Sera of Patients with Idiopathic Pulmonary Fibrosis

Wensheng Chen[*], **Tejas R. Karhadkar**[*], **Changwan Ryu**[†], **Erica L. Herzog**[†], **Richard H. Gomer**[*]

[*]Department of Biology, Texas A&M University, College Station, TX 77843;

[†]Section of Pulmonary, Critical Care and Sleep Medicine, Yale School of Medicine, New Haven, CT 06510

Abstract

Pulmonary fibrosis is a chronic and generally fatal disorder characterized by progressive formation of scar-like tissue in the lungs. Sialic acids are often found as the terminal sugar on extracellular glycoconjugates such as protein glycosylations. Sialidases, also known as neuraminidases, desialylate glycoconjugates. Serum amyloid P (SAP), a pentameric serum glycoprotein that has two sialic acids on each polypeptide, inhibits the differentiation of monocytes into fibrocytes and promotes human PBMCs to accumulate high extracellular levels of IL-10. When SAP is desialylated with sialidase, the effects of SAP on fibrocyte differentiation and IL-10 accumulation are strongly inhibited. Intriguingly, in patients with pulmonary fibrosis, there are increased levels of sialidase activity in the bronchoalveolar lavage fluid, increased levels of sialidases in the lungs, and decreased levels of SAP in the sera. To elucidate the role of SAP desialylation in idiopathic pulmonary fibrosis (IPF) pathogenesis, we purified SAP from the serum of IPF patients and healthy controls and measured the extent of sialylation and bioactivity of the purified SAP. We find that some IPF patients have abnormally high levels of the sialidase NEU3 in their sera and that the SAP in the sera of IPF patients has an abnormally high extent of desialylation and an abnormally low ability to inhibit fibrocyte differentiation and induce extracellular IL-10 accumulation by PBMC. These results suggest that SAP desialylation may play a role in IPF pathogenesis and that inhibiting NEU3 could be a potential therapeutic target for IPF. *ImmunoHorizons*, 2020, 4: 352–362.

INTRODUCTION

Fibrosing diseases, such as idiopathic pulmonary fibrosis (IPF), cirrhosis, and end-stage kidney disease, involve a progressive formation of scar tissue in internal organs that replaces

Address correspondence and reprint requests to: Dr. Richard H. Gomer, Department of Biology, Texas A&M University, 301 Old Main Drive, College Station, TX 77843-3474. rgomer@tamu.edu.

DISCLOSURES
The authors have no financial conflicts of interest.

The online version of this article contains supplemental material.

the normal tissue, causing organ failure and 30–45% of deaths in the United States (1). Fibrosis involves prolonged or recurrent structural cell injury, infiltration of blood leukocytes into the affected organs, activation and/or appearance of fibroblasts and fibroblast-like cells, and deposition of extracellular matrix proteins such as collagen (2). The mechanisms that allow fibrosis to continue to form scar tissue, rather than to stop as in normal wound healing, are poorly understood.

Sialic acids are often found as the terminal sugar on extracellular glycoconjugates such as protein glycosylations (3, 4). Sialidases (also known as neuraminidases) remove sialic acid from glycoconjugates. Serum amyloid P (SAP), a pentameric serum glycoprotein that has two sialic acids on each polypeptide, inhibits the differentiation of monocytes into fibroblast-like cells called fibrocytes (5, 6), potentiates cultures of PBMCs to accumulate high extracellular levels of the anti-inflammatory cytokine IL-10 (7, 8), and inhibits fibrosis in animal models and a phase 2 clinical trial in patients with IPF (9–12). In part because of its sialylation, SAP binds to the lectin receptor DC-SIGN (13). When SAP is desialylated with sialidase, there is decreased SAP binding to macrophages, dendritic cells, and monocytes, and the effects of SAP on fibrocyte differentiation and pro–IL-10 accumulation are strongly inhibited (13). In addition, desialylated SAP is rapidly cleared from the circulation in humans (14, 15). Intriguingly, in patients with pulmonary fibrosis, there are increased levels of sialidase activity in the bronchoalveolar lavage fluid, increased levels of sialidases in the lungs (16–19), and decreased levels of SAP in the sera (7). Mice lacking the sialidase NEU3 develop very little fibrosis in the standard bleomycin model, suggesting that NEU3 plays a role in fibrosis (19). In this report, we find that some IPF patients have abnormally high levels of NEU3 in their sera and that the SAP in the serum of IPF patients has an abnormally high extent of desialylation and an abnormally low ability to inhibit fibrocyte differentiation and induce extracellular IL-10 accumulation by PBMC.

MATERIALS AND METHODS

Serum samples

Serum samples from deidentified healthy controls, stable IPF, and progressive IPF patients were collected at the Yale School of Medicine with approval from the Yale Institutional Review Board and with written consent from the donors. For IPF patients, inclusion and exclusion criteria were as described in the European Respiratory Society/American Thoracic Society consensus statement (20). Comprehensive clinical data (21), including age, sex, race and ethnicity, comorbidities, medications, and physiologic impairment as measured by the percentage of predicted forced vital capacity (FVC%) and percentage of diffusion capacity of carbon monoxide (DLCO%), were collected. IPF subjects were considered “progressive” if they died of any cause within 2 y of blood draw. Subjects were designated as “stable” if they were alive after 2 y (22, 23). Moreover, we also used the Gender, Age, and Physiology (GAP) index score as a check for IPF disease severity. This is a widely used measure of IPF severity that provides validated prognostic data on IPF subjects (21). Not surprisingly, the progressive subjects had an elevated GAP index score, indicating that they had severe disease with a higher risk of mortality. Age-matched normal controls were recruited from the local community. The serum samples were stored at −80°C.

Serum protein, SAP, and NEU3 quantitation

Serum samples were thawed overnight at 4°C. Serum protein concentration was measured by OD 280/260 with a Synergy Mx plate reader (BioTek, Winooski, VT) with a Take3 Multi-Volume Plate insert and Gen5 Take3 software module and reading at 260, 280, and 320 nm to correct for nucleic acids and particulate matter, with 0.9% saline as a blank. Serum SAP concentration was measured as described previously (5). Serum NEU3 was measured as described previously (18), with the following modifications. Sera were diluted to a final concentration of 100 μg protein/well in 50 μl of PBS in a 96-well MaxiSorp Immune Plate (no. 442402; Thermo Fisher Scientific, Waltham, MA) and incubated at 4°C overnight. Serial dilutions of recombinant human NEU3 (no. TP316537; OriGene, Rockville, MD) were also incubated and used for a standard curve. The solutions were removed, and the wells were blocked with 200 μl 2% BSA in PBS for 2 h at room temperature with shaking. Anti-human NEU3 Abs (no. 21630002; Novus Biologicals, Littleton, CO) were then added in 2% BSA/PBS for 3 h at room temperature, following the manufacturer's directions. After washing, 1:1000 HRP-conjugated donkey anti-rabbit IgG (The Jackson Laboratory, Philadelphia, PA) in 2% BSA/PBS was added for 2 h. After washing, bound Abs were detected using a TMB Color Development Kit (BioLegend, San Diego, CA), and the reaction was stopped with 1 N HCl. Absorbances at 450 and 550 nm were measured using a Synergy Mx plate reader (BioTek).

SAP purification, SAP desialylation, and SAP resialylation

SP Sepharose Fast Flow beads (GE Healthcare Life Sciences, Piscataway, NJ) were washed three times with 10-bead volumes of binding buffer (20 mM Tris [pH 8.0], 140 mM NaCl, and 2 mM $CaCl_2$) before use (24–26). Then, 1 ml of serum, 200 μl of binding buffer, and 300 μl of SP Sepharose Fast Flow beads were mixed overnight at 4°C with gentle shaking. The beads were collected by centrifugation at 300 × *g* for 1 min, and the supernatant was removed. Three milliliters of binding buffer was added to the beads and mixed on a rotator for 5 min at room temperature. The beads were then washed four times with 3 ml wash buffer (20 mM Tris [pH 8], 400 mM NaCl, and 2 mM $CaCl_2$) by mixing for 5 min and centrifugation at 300 × *g* for 1 min. After removing the supernatant from the fourth wash, 300 μl of elution buffer (20 mM Tris [pH 8], 140 mM NaCl, and 50 mM EDTA [pH 8]) was added to the beads and mixed for 1 h at room temperature. After centrifugation at 300 × *g* for 1 min, the supernatant (first elution), which contained SAP, was collected. The elution step was repeated once by adding 300 μl fresh elution buffer and mixing for 30 min at room temperature. The second elution was collected and combined with the first elution. The combined elutions were buffer exchanged and concentrated five times at 10,000 × *g* with a 100-kDa cutoff of Amicon Ultra-0.5 mL Centrifugal Filter (MilliporeSigma), following the manufacturer's instructions. The SAP used for mass spectrometry was buffer exchanged into water, whereas the SAP used for cell experiments was buffer exchanged to 20 mM sodium phosphate buffer (pH 7.4). The SAP concentration was measured as described above for serum protein concentrations. SAP was incubated with sialidase from Arthrobacter (Sigma, St. Louis, MO) at 37°C for 24 h, following the manufacturer's protocol. The desialylated SAP (a 127 kDa pentamer) was buffer exchanged as above with a 100 kDa cutoff spin filter into 20 mM sodium phosphate (pH 7.4) or water to remove the 88 kDa sialidase and reaction products. SAP was sialylated or resialylated with CMP-NANA (Sigma) and α (2,

6) sialyltransferase (Sigma) at 37°C for 4 h following the manufacturer's protocol and then buffer exchanged as above into 20 mM sodium phosphate or water to remove the 50 kDa sialyltransferase and the CMP-NANA.

Western blots and silver staining

Serum samples were diluted 1:100 in 20 mM sodium phosphate (pH 7.4). Then, 5 μl of diluted serum was mixed with 5 μl of 2× protein sample buffer and heated at 95°C for 10 min. SDS-PAGE was done following (5). For analysis of biotinylated peanut agglutinin (PNA; Vector Laboratories, Burlingame, CA) and biotinylated *Sambucus nigra* lectin (SNA; Vector Laboratories) staining, Western blots were preincubated with Carbo-Free Blocking Solution (Vector Laboratories) and then incubated with biotinylated PNA or SNA diluted in the same carbo-free solution at 2 μg/ml for 30 min at room temperature. For SAP staining, Western blots were incubated with 1 μg/ml rabbit anti-SAP Ab (Sigma) overnight at 4°C. Labeling was detected with streptavidin–HRP (BioLegend), as described previously (27). Purified and modified SAP samples were stained with silver nitrate (28) after SDS-PAGE.

Mass spectrometry

Commercially available purified human SAP (Fitzgerald Industries, Acton, MA) or SAP purified as described above were buffer exchanged into water and diluted with organic electrospray solvent to a final ratio of 50% acetonitrile (Thermo Fisher Scientific, Fair Lawn, NJ) and 1% formic acid (Agilent Technologies, Santa Clara, CA) at a concentration of ~10 μM SAP monomer for mass spectrometry. Three microliters of SAP samples were loaded into a single-use glass tip (Sutter Health, Novato, CA) and delivered to the mass spectrometer via Nano-electrospray. Voltage of 1300 V was applied through a platinum wire insert. The ion transfer tube temperature was set to 250°C. Mass spectrometric analysis was carried out on an Orbitrap Fusion instrument (Thermo Fisher Scientific, Bremen, Germany) equipped with a Nanospray Flex offline static spray source (Thermo Fisher Scientific). All SAP samples were analyzed in the Orbitrap at a resolution of 120,000 at m/z 400. The monitored m/z range was 1200–2000; the quadrupole was set to isolation mode in the same m/z range to improve the signal-to-noise ratio of the peaks of interest. Ten microscans were summed per scan. Data were acquired for a minimum of 3 min. Deconvolution of mass spectra was performed by the use of UniDec software (29) in the 24,600–25,600 Da mass range. Sialic acids on SAP monomer were quantified based on the relative absorbance at 25,462 Da (with two sialic acids), 25,171 Da (with one sialic acid), and 24,880 Da (with no sialic acid).

PBMC isolation and culture, fibrocyte counts, and IL-10 assay

Human peripheral blood was collected into heparin tubes (BD Biosciences, San Jose, CA) from healthy adult volunteers who gave written consent and with specific approval from the Texas A&M University human subjects Institutional Review Board. PBMCs were isolated from the blood using Ficoll Paque Plus (GE Healthcare) and cultured, as described previously (6). Then, 5×10^5 cells/ml PBMCs were cultured in serum-free medium in the presence or absence of purified SAP or raw serum from healthy controls and IPF patients for 5 d at 37°C. Culture supernatants were removed and stored at −20°C, cells were fixed and stained, and fibrocytes were counted, as described previously (30). The day 5 culture supernatants were analyzed with a human IL-10 ELISA kit (BioLegend), following the manufacturer's directions. The IC_{50} of SAP and raw serum on fibrocyte differentiation was generated by fitting a sigmoidal dose-response curve with variable Hill coefficient to the combined data from three separate assays for each patient. SAP- and raw serum–induced IL-10 concentrations were fitted to a second-order polynomial curve, using only the data from the control up to the first data point that was higher than twice the control value, defining EC2 as the concentration (in percentage) of serum needed to double the concentration of extracellular IL-10, and the EC2 was calculated according to the equation of the curve.

Statistics

All assays were done at least three independent times. For assays with cells, three different donors were used. Parameters used for correlation analysis are listed in Supplemental Table I. For values corresponding to groups of patients, the mean for each patient was calculated. These means (8 controls, 10 stable, and 10 progressive IPF patients, or 20 combined IPF patients) were then averaged to get the final mean, and the SEM of the 8, 10, or 20 values was then calculated and is presented as the SEM. Data were analyzed by *t* test or ANOVA using Prism software (GraphPad, La Jolla, CA).

RESULTS

Serum from IPF patients contains more NEU3 and more desialylated proteins

Sialic acid is a monosaccharide located at the terminal positions of glycoconjugates (3, 31). Sialidases, also known as neuraminidases, remove the terminal sialic acid (desialylation) from these glycoconjugates (17, 32). The desialylation of glycoproteins induces multiple functional changes in immunity (4, 33, 34). Sialidases such as NEU3 are elevated in the lungs of patients with pulmonary fibrosis (16–18). To determine if NEU3 can be detected in the serum of pulmonary fibrosis patients, serum samples from 8 healthy controls, 10 stable IPF patients, and 10 progressive IPF patients (Table I) were assayed for NEU3 by ELISA. There were no significant differences between stable and progressive IPF patients in FVC%, DLCO%, and GAP index. The serum protein concentrations of patients and controls ranged from 44.7 ± 10.2 to 58.9 ± 0.5 mg/ml (mean ± SEM, $n = 3$), with no serum protein concentrations significantly different from any other (one-way ANOVA, both Tukey test and Bonferroni test). Coomassie Blue–stained gels of these serum samples also indicated that there were approximately equal serum protein concentrations (Fig. 1A). There were also no significant differences in the mean serum protein concentrations of the three groups (stable, progressive, and control; one-way ANOVA, both Tukey test and Bonferroni test). NEU3 increased in the serum of some IPF patients compared with healthy controls (Fig. 1B). Serum NEU3 inversely correlated with DLCO% (Supplemental Fig. 1) but not FVC% (Supplemental Fig. 1) or GAP (Supplemental Fig. 1).

To determine if there is abnormal sialylation of serum components in pulmonary fibrosis, the above serum samples were electrophoresed on SDS-PAGE gels, and Western blots were stained with PNA and SNA, which detects nonsialylated carbohydrates (35) and sialylated carbohydrates (36) (Fig. 1A). Sera from IPF patients tended to show more PNA staining and less SNA staining (integrated over all the bands in the gel) than healthy controls, and sera from patients with progressive IPF showed more PNA staining than sera from patients with stable IPF (Fig. 1A, 1C, 1D). For the IPF patients, the integrated PNA staining intensity of serum samples inversely correlated with FVC% (Supplemental Fig. 1) and correlated with serum NEU3 concentrations (Supplemental Fig. 1). SNA staining intensity correlated with FVC% (Supplemental Fig. 1), DLCO% (Supplemental Fig. 1), and total serum protein levels (Supplemental Fig. 1) and inversely correlated with serum NEU3 concentrations (Supplemental Fig. 1) and PNA staining intensity (Supplemental Fig. 1).

Serum from IPF patients has less SAP, and the SAP is more desialylated

The serum glycoprotein SAP, which has two α (2, 6)-linked terminal sialic acids on each ~26 kDa monomer and thus 10 sialic acids on the pentamer (15), appears to have a calming effect on the innate immune system and inhibits fibrosis in animal models and in clinical trials (9, 37–39). The terminal sialic acid on SAP plays a key role in its ability to regulate the innate immune system, and when SAP is desialylated with sialidases, the effects of SAP are largely abrogated (13). Patients with measles, systemic sclerosis, mixed connective tissue disease, primary myelofibrosis, hepatitis, liver fibrosis, and IPF tend to have less SAP in the serum compared with healthy controls (7, 24, 40–42). In addition, a decrease of serum SAP was found in progressive diastolic dysfunction patients compared with more stable patients (43). In agreement with the previous results, using an ELISA with Abs against specific peptide domains SAP, and thus unaffected by the sialylation state of SAP, IPF patient sera contained less SAP than healthy controls (Fig.2A).

As a partial test of the hypothesis that the high levels of sialidases observed in pulmonary fibrosis cause SAP desialylation, we purified SAP from the serum samples (Supplemental Fig. 2) and measured the sialic acid on each SAP monomer by mass spectrometry (Supplemental Fig. 3). The mass of SAP with two sialic acids is 25,462 Da (44). SAP masses of 25,171 and 24,880 Da have also been observed (15), corresponding to the loss of one or both of the terminal sialic acids: one *N*-acetylneuraminic acid removed and one hydroxyl (−OH) added, leading to a net 291 Da loss for each sialic acid removed. In agreement with the previously published results, we also observed by mass spectrometry material at 24,880, 25,171, and 25,462 Da in samples of SAP purified from human serum (Supplemental Fig. 3).

To verify that the peaks identified as being sialylated SAP are indeed sialylated, commercial human SAP or SAP purified from the sera of four healthy control patients was desialylated with sialidase, and we observed that the 25,462 and 25,171 Da peaks identified as sialidated SAP decreased or disappeared (Supplemental Figs. 2B, 2C, 3). Treatment of the desialylated commercial SAP or SAP purified from five IPF patients with sialyltransferase and sialic acid caused a reappearance or increase of the sialidated SAP peaks, further verifying the identification of the 25,462 and 25,171 Da peaks as being sialidated (Supplemental Figs. 2B, 2D, 3).

Compared with the SAP purified from the sera of healthy controls, SAP from the sera of IPF patients tended to have less sialic acid (Supplemental Figs. 2E, 3). Together, these results indicate that the SAP in the sera of IPF patients tends to have less sialylation than the SAP in the sera of control patients. Serum SAP concentration correlated with FVC% (Supplemental Fig. 1), DLCO% (Supplemental Fig. 1), and SNA staining intensity (Supplemental Fig. 1) and inversely correlated with serum NEU3 (Supplemental Fig. 1) and PNA staining (Supplemental Fig. 1). SAP sialylation correlated with FVC% (Supplemental Fig. 1), SNA staining intensity (Supplemental Fig. 1), and serum SAP concentration (Supplemental Fig. 1) and inversely correlated with DLCO% (Supplemental Fig. 1), serum NEU3 (Supplemental Fig. 1), and PNA staining (Supplemental Fig. 1).

SAP from IPF patients has abnormally low bioactivity

Fibrocytes are $CD45^+$/collagen I^+ fibroblast-like cells that share characteristics of both hematopoietic and stromal cells (45). Fibrocytes are found in healing dermal wounds and fibrotic lesions and secrete collagen and enzymes that modify the extracellular matrix (46). In serum-free media, some blood monocytes differentiate into fibrocytes, and SAP inhibits this differentiation (5, 30). IL-10 is an anti-inflammatory cytokine, and SAP promotes the accumulation of extracellular IL-10 by macrophages (8, 13). To determine if SAP purified from the sera of IPF patients has an abnormal bioactivity, we treated human PBMCs from healthy volunteers for 5 d with the SAP that we purified from controls and patients. Fibrocyte numbers were counted, and IL-10 levels in the culture supernatants were assayed by ELISA. A commercial human SAP purchased from Fitzgerald Industries (Fitz-SAP) was used as a positive control in the assays. In the fibrocyte differentiation and IL-10 assays, SAP purified from the sera of healthy controls showed effects similar to the effects of the commercially available SAP and to previously published data (13, 30, 39), whereas the SAP from IPF patients showed a less inhibitory effect on fibrocyte differentiation and inducedless IL-10 accumulation than SAP from healthy controls (Fig. 3A, 3B). The IC_{50} of SAP purified from IPF sera on fibrocyte differentiation was higher than that of SAP purified from healthy controls (0.84 ± 0.05 versus 0.38 ± 0.03 μg/ml; mean ± SEM, $n = 3$, $p < 0.0001$ [t test]), and Fitz-SAP showed a similar IC_{50} to control serum SAP (0.33 ± 0.02 μg/ml). Defining EC2 as the concentration of SAP needed to double the concentration of extracellular IL-10, the EC2 of IPF serum SAP on IL-10 accumulation was higher than that of control serum SAP (2.61 ± 0.25 versus 0.28 ± 0.06 μg/ml; mean ± SEM, $n = 3$, $p < 0.0001$ [t test]), and Fitz-SAP showed a similar EC2 to control serum SAP (0.25 ± 0.04 μg/ml; mean ± SEM, $n = 3$).

The IC_{50} of SAP on fibrocyte differentiation correlated with serum NEU3 (Supplemental Fig. 1) and PNA staining (Supplemental Fig. 1) and inversely correlated with DLCO% (Supplemental Fig. 1), SNA staining (Supplemental Fig. 1), serum SAP (Supplemental Fig. 1), and SAP sialylation (Supplemental Fig. 1). The EC2 of SAP on IL-10 accumulation correlated with serum NEU3 (Supplemental Fig. 1), PNA staining (Supplemental Fig. 1), and IC_{50} of SAP on fibrocyte differentiation (Supplemental Fig. 1) and inversely correlated with FVC% (Supplemental Fig. 1), DLCO% (Supplemental Fig. 1), SNA staining (Supplemental Fig. 1), serum SAP (Supplemental Fig. 1), and SAP sialylation (Supplemental Fig. 1).

Desialylation of SAP from healthy controls and resialylation of SAP from IPF patients reverse their effects on fibrocyte differentiation and IL-10 accumulation

To test the hypothesis that the abnormally low bioactivity of SAP from IPF patients is due to its abnormally high desialylation, we desialylated SAP from healthy controls (De-Con-SAP), resialylated some of this SAP, sialylated SAP from IPF patients, and tested their effects on PBMCs. Compared with SAP from healthy controls, desialylated control SAP showed less of an effect on inhibiting fibrocyte differentiation and promoting IL-10 accumulation (Fig. 4A, 4B). Resialylation of the desialylated control SAP restored the SAP bioactivity (Fig. 4A, 4B). Conversely, sialylation of IPF patient SAP increased the ability of this SAP to inhibit fibrocyte differentiation and to promote IL-10 accumulation (Fig. 4C, 4D). There was no discernable effect of any of the materials added to cells on viability or cell numbers during the experiments. These results suggest that the abnormally low bioactivity of IPF patient SAP is due to its abnormally low level of sialylation.

Serum from IPF patients has abnormally low bioactivity

A concentration of 0.1% or higher of human serum significantly decreases fibrocyte differentiation, and this effect is lost when SAP is depleted from the serum (5). Consistent with the previous results showing that IPF patients have abnormally low levels of serum SAP (7), raw sera from IPF patients showed less of an inhibitory effect on fibrocyte differentiation than control sera (Fig. 5A), and IPF patient sera induced less extracellular IL-10 accumulation than control sera (Fig. 5B). The IC_{50} of IPF patient sera on fibrocyte differentiation was higher than that of control sera (0.102 ± 0.004% versus 0.037 ± 0.003%; mean ± SEM, $n = 3$, $p < 0.0001$ [*t* test]). Defining EC2 as the concentration (in percentage) of serum needed to double the concentration of extracellular IL-10, the EC2 of raw IPF serum on IL-10 accumulation was higher than the raw control serum (0.16 ± 0.02% versus 0.015 ± 0.003%; mean ± SEM, $n = 3$, $p < 0.001$ [*t* test]).

The IC_{50} of raw serum on fibrocyte differentiation correlated with serum NEU3 (Supplemental Fig. 1), PNA staining (Supplemental Fig. 1), the IC_{50} of SAP on fibrocyte differentiation (Supplemental Fig. 1), and the EC2 of SAP on IL-10 accumulation (Supplemental Fig. 1) and inversely correlated with FVC% (Supplemental Fig. 1), SNA staining (Supplemental Fig. 1), serum SAP (Supplemental Fig. 1), and SAP sialylation (Supplemental Fig. 1). The EC2 of raw serum on IL-10 accumulation correlated with serum NEU3 (Supplemental Fig. 1), PNA staining (Supplemental Fig. 1), the IC_{50} of SAP on fibrocyte differentiation (Supplemental Fig. 1), the EC2 of SAP on IL-10 accumulation (Supplemental Fig. 1), and the IC_{50} of raw serum on fibrocyte differentiation (Supplemental Fig. 1) and inversely correlated with SNA staining (Supplemental Fig. 1), serum SAP (Supplemental Fig. 1), and SAP sialylation (Supplemental Fig. 1).

Because the major inhibitor of fibrocyte differentiation in serum is SAP (5), for each patient, the IC_{50} for purified SAP inhibiting fibrocyte differentiation, divided by the serum SAP concentration for that patient, should be roughly equal to the IC_{50} for the raw serum from that patient, inhibiting fibrocyte differentiation. As shown in Supplemental Fig. 1, this rough correlation appears to hold. Similarly, for each patient, the EC2 of SAP on IL-10 accumulation/serum SAP showed a rough correlation to the EC2 of raw serum on IL-10 accumulation (Supplemental Fig. 1).

DISCUSSION

In this report, we observed abnormally high levels of NEU3 in the sera of some IPF patients. NEU3 is present on the extracellular side of the plasma membrane and can be released from cells (47–49). Combined with our previous observation of high levels of NEU3 in the fibrotic lesions of IPF patients (18), this suggests that in some IPF patients, NEU3 from fibrotic lesions can leak into the blood. Whether this NEU3 in the serum is bioactive is, however, unknown.

IPF patients tended to have increased levels of serum protein desialylation and increased levels of SAP desialylation. Both of these showed some, but not perfect, correlation with serum NEU3 levels, suggesting that the serum protein and serum SAP desialylation is due to a combination of the elevated NEU3 in fibrotic lesions and the serum. Other sialidases are also upregulated in pulmonary fibrosis, so these sialidases may also be responsible for desialylating SAP (16, 18, 19). Whether the desialylation of SAP occurs in the lungs, in the circulation, or in some other tissue is unknown. Because desialylated SAP is rapidly cleared from the blood in humans (14, 15), the low serum SAP levels in IPF patients (7) that we also observed may be due to SAP desialylation.

Compared with healthy donor SAP, IPF patient SAP had a poor ability to inhibit fibrocyte differentiation or increase IL-10 accumulation, and this could be reversed by sialylating the IPF patient SAP and mimicked by desialylating control SAP. The poor ability to inhibit fibrocyte differentiation and increase IL-10 accumulation was also observed for the sera of IPF patients. With the assumption that fibrocytes are profibrotic and IL-10 is antifibrotic, this indicates that IPF patients experience two parallel profibrotic mechanisms: low levels of SAP and the SAP that is there has poor bioactivity. Together, these results suggest SAP desialylation may play a role in IPF pathogenesis.

We previously found that the profibrotic cytokine TGF-β1 upregulates NEU3 and that NEU3 upregulates TGF-β1, suggesting the existence of a potential positive feedback loop in fibrosis (18, 19). From engineering principles, positive feedback loops can dramatically increase the response time and sensitivity of a system. To upregulate NEU3, instead of a conventional increase in transcription, cells responsive to TGF-β1 already have *NEU3* mRNA in their cytosol but keep much of it out of polysomes and, in response to TGF-β1, increase the translation of the existing *NEU3* mRNA, suggesting a rapid response (50). We previously found that NEU3 inactivates SAP bioactivity (18) and that SAP inhibits wound healing (26). One effect of this rapid TGF-β1–NEU3–TGF-β1 feedback loop would thus be to inactivate SAP. Together, these effects may have evolved to potentiate a rapid response to wounding or other damage and a rapid initiation of wound healing.

Fibrosis appears to involve this feedback loop and other feedback loops, stuck in a gain >1 state, in which the pathway components are continuously activating each other. Given the success of SAP therapy in inhibiting IPF in phase 2 trials and the observed deleterious effect of IPF-associated desialylation on SAP, inhibiting NEU3 to inhibit SAP desialylation could be a potential therapeutic target for IPF.

Supplementary Material

Refer to Web version on PubMed Central for supplementary material.

ACKNOWLEDGMENTS

We thank Klaudia I. Kocurek for the mass spectrometry work and writing the mass spectrometry method section and Darrell Pilling for helpful comments.

This work was supported by National Institutes of Health HL118507 (to R.H.G.) and HL109233 (to E.L.H.).

Abbreviations used in this article:

De-Con-SAP	desialylated SAP from healthy control
DLCO%	percentage of diffusion capacity of carbon monoxide
Fitz-SAP	a commercial human SAP purchased from Fitzgerald Industries
FVC%	percentage of predicted forced vital capacity
GAP	Gender, Age, and Physiology
IPF	idiopathic pulmonary fibrosis
PNA	peanut agglutinin
SAP	serum amyloid P
SNA	*Sambucus nigra* lectin

REFERENCES

1. Duffield JS, Lupher M, Thannickal VJ, and Wynn TA. 2013. Host responses in tissue repair and fibrosis. Annu. Rev. Pathol 8: 241–276. [PubMed: 23092186]
2. King TE Jr., Pardo A, and Selman M. 2011. Idiopathic pulmonary fibrosis. Lancet 378: 1949–1961. [PubMed: 21719092]
3. Bate C, Nolan W, McHale-Owen H, and Williams A. 2016. Sialic acid within the glycosylphosphatidylinositol anchor targets the cellular prion protein to synapses. J. Biol. Chem 291: 17093–17101. [PubMed: 27325697]
4. Mahajan VS, and Pillai S. 2016. Sialic acids and autoimmune disease. Immunol. Rev 269: 145–161. [PubMed: 26683151]
5. Pilling D, Buckley CD, Salmon M, and Gomer RH. 2003. Inhibition of fibrocyte differentiation by serum amyloid P. J. Immunol 171: 5537–5546. [PubMed: 14607961]
6. Pilling D, Vakil V, and Gomer RH. 2009. Improved serum-free culture conditions for the differentiation of human and murine fibrocytes. J. Immunol. Methods 351: 62–70. [PubMed: 19818792]
7. Murray LA, Chen Q, Kramer MS, Hesson DP, Argentieri RL, Peng X, Gulati M, Homer RJ, Russell T, van Rooijen N, et al. 2011. TGF-beta driven lung fibrosis is macrophage dependent and blocked by Serum amyloid P. Int. J. Biochem. Cell Biol 43: 154–162. [PubMed: 21044893]

8. Zhang W, Xu W, and Xiong S. 2011. Macrophage differentiation and polarization via phosphatidylinositol 3-kinase/Akt-ERK signaling pathway conferred by serum amyloid P component. J. Immunol 187: 1764–1777. [PubMed: 21753147]

9. Raghu G, van den Blink B, Hamblin MJ, Brown AW, Golden JA, Ho LA, Wijsenbeek MS, Vasakova M, Pesci A, Antin-Ozerkis DE, et al. 2018. Effect of recombinant human pentraxin 2 vs placebo on change in forced vital capacity in patients with idiopathic pulmonary fibrosis: a randomized clinical trial. JAMA 319: 2299–2307. [PubMed: 29800034]

10. Raghu G, van den Blink B, Hamblin MJ, Brown AW, Golden JA, Ho LA, Wijsenbeek MS, Vasakova M, Pesci A, Antin-Ozerkis DE, et al. 2019. Long-term treatment with recombinant human pentraxin 2 protein in patients with idiopathic pulmonary fibrosis: an open-label extension study. Lancet Respir. Med 7: 657–664. [PubMed: 31122893]

11. Pilling D, Roife D, Wang M, Ronkainen SD, Crawford JR, Travis EL, and Gomer RH. 2007. Reduction of bleomycin-induced pulmonary fibrosis by serum amyloid P. J. Immunol 179: 4035–4044. [PubMed: 17785842]

12. Haudek SB, Xia Y, Huebener P, Lee JM, Carlson S, Crawford JR, Pilling D, Gomer RH, Trial J, Frangogiannis NG, and Entman ML. 2006. Bone marrow-derived fibroblast precursors mediate ischemic cardiomyopathy in mice. Proc. Natl. Acad. Sci. USA 103: 18284–18289. [PubMed: 17114286]

13. Cox N, Pilling D, and Gomer RH. 2015. DC-SIGN activation mediates the differential effects of SAP and CRP on the innate immune system and inhibits fibrosis in mice. Proc. Natl. Acad. Sci. USA 112: 8385–8390. [PubMed: 26106150]

14. Siebert H-C, André S, Reuter G, Gabius H-J, Kaptein R, and Vliegenthart JFG. 1995. Effect of enzymatic desialylation of human serum amyloid P component on surface exposure of laser photo CIDNP (chemically induced dynamic nuclear polarization)--reactive histidine, tryptophan and tyrosine residues. FEBS Lett. 371: 13–16. [PubMed: 7664874]

15. Pepys MB, Rademacher TW, Amatayakul-Chantler S, Williams P, Noble GE, Hutchinson WL, Hawkins PN, Nelson SR, Gallimore JR, Herbert J, et al. 1994. Human serum amyloid P component is an invariant constituent of amyloid deposits and has a uniquely homogeneous glycostructure. Proc. Natl. Acad. Sci. USA 91: 5602–5606. [PubMed: 8202534]

16. Luzina IG, Lockatell V, Hyun SW, Kopach P, Kang PH, Noor Z, Liu A, Lillehoj EP, Lee C, Miranda-Ribera A, et al. 2016. Elevated expression of NEU1 sialidase in idiopathic pulmonary fibrosis provokes pulmonary collagen deposition, lymphocytosis, and fibrosis. Am. J. Physiol. Lung Cell. Mol. Physiol 310: L940–L954. [PubMed: 26993524]

17. Lambré CR, Pilatte Y, Le Maho S, Greffard A, De Crémoux H, and Bignon J. 1988. Sialidase activity and antibodies to sialidase-treated autologous erythrocytes in bronchoalveolar lavages from patients with idiopathic pulmonary fibrosis or sarcoidosis. Clin. Exp. Immunol 73: 230–235. [PubMed: 3180512]

18. Karhadkar TR, Pilling D, Cox N, and Gomer RH. 2017. Sialidase inhibitors attenuate pulmonary fibrosis in a mouse model. Sci. Rep 7: 15069. [PubMed: 29118338]

19. Karhadkar TR, Chen W, and Gomer RH. 2020. Attenuated pulmonary fibrosis in sialidase-3 knockout ($Neu3^{-/-}$) mice. Am. J. Physiol. Lung Cell. Mol. Physiol 318: L165–L179. [PubMed: 31617733]

20. Raghu G, Collard HR, Egan JJ, Martinez FJ, Behr J, Brown KK, Colby TV, Cordier JF, Flaherty KR, Lasky JA, et al. ; ATS/ERS/JRS/ALAT Committee on Idiopathic Pulmonary Fibrosis. 2011. An official ATS/ERS/JRS/ALAT statement: idiopathic pulmonary fibrosis: evidence-based guidelines for diagnosis and management. Am. J. Respir. Crit. Care Med 183: 788–824. [PubMed: 21471066]

21. Ley B, Ryerson CJ, Vittinghoff E, Ryu JH, Tomassetti S, Lee JS, Poletti V, Buccioli M, Elicker BM, Jones KD, et al. 2012. A multidimensional index and staging system for idiopathic pulmonary fibrosis. Ann. Intern. Med 156: 684–691. [PubMed: 22586007]

22. King TE Jr., Albera C, Bradford WZ, Costabel U, du Bois RM, Leff JA, Nathan SD, Sahn SA, Valeyre D, and Noble PW; Implications for the Design and Execution of Clinical Trials. 2014. All-cause mortality rate in patients with idiopathic pulmonary fibrosis. Implications for the design and execution of clinical trials. Am. J. Respir. Crit. Care Med 189: 825–831. [PubMed: 24476390]

23. Meyer KC, Raghu G, Baughman RP, Brown KK, Costabel U, du Bois RM, Drent M, Haslam PL, Kim DS, Nagai S, et al. ; American Thoracic Society Committee on BAL in Interstitial Lung Disease. 2012. An official American Thoracic Society clinical practice guideline: the clinical utility of bronchoalveolar lavage cellular analysis in interstitial lung disease. Am. J. Respir. Crit. Care Med 185: 1004–1014. [PubMed: 22550210]
24. Mantovaara T, Pertoft H, and Porath J. 1989. Purification of human serum amyloid P component (SAP) by calcium affinity chromatography. Biotechnol. Appl. Biochem 11: 564–570. [PubMed: 2597355]
25. Hind CR, Collins PM, Renn D, Cook RB, Caspi D, Baltz ML, and Pepys MB. 1984. Binding specificity of serum amyloid P component for the pyruvate acetal of galactose. J. Exp. Med 159: 1058–1069. [PubMed: 6707579]
26. Gomer RH, Pilling D, Kauvar LM, Ellsworth S, Ronkainen SD, Roife D, and Davis SC. 2009. A serum amyloid P-binding hydrogel speeds healing of partial thickness wounds in pigs. Wound Repair Regen. 17: 397–404. [PubMed: 19660048]
27. Pilling D, and Gomer RH. 2014. Persistent lung inflammation and fibrosis in serum amyloid P component (APCs$^{-/-}$) knockout mice. PLoS One 9: e93730. [PubMed: 24695531]
28. Morrissey JH 1981. Silver stain for proteins in polyacrylamide gels: a modified procedure with enhanced uniform sensitivity. Anal. Biochem 117: 307–310. [PubMed: 6172996]
29. Marty MT, Baldwin AJ, Marklund EG, Hochberg GKA, Benesch JLP, and Robinson CV. 2015. Bayesian deconvolution of mass and ion mobility spectra: from binary interactions to polydisperse ensembles. Anal. Chem 87: 4370–4376. [PubMed: 25799115]
30. Cox N, Pilling D, and Gomer RH. 2014. Distinct Fcγ receptors mediate the effect of serum amyloid p on neutrophil adhesion and fibrocyte differentiation. J. Immunol 193: 1701–1708. [PubMed: 25024390]
31. Schauer R 2009. Sialic acids as regulators of molecular and cellular interactions. Curr. Opin. Struct. Biol 19: 507–514. [PubMed: 19699080]
32. Varki A, and Gagneux P. 2012. Multifarious roles of sialic acids in immunity. Ann. N. Y. Acad. Sci 1253: 16–36. [PubMed: 22524423]
33. Kubota M, Takeuchi K, Watanabe S, Ohno S, Matsuoka R, Kohda D, Nakakita S-I, Hiramatsu H, Suzuki Y, Nakayama T, et al. 2016. Trisaccharide containing α2,3-linked sialic acid is a receptor for mumps virus. Proc. Natl. Acad. Sci. USA 113: 11579–11584. [PubMed: 27671656]
34. Pawluczyk IZA, Ghaderi Najafabadi M, Patel S, Desai P, Vashi D, Saleem MA, and Topham PS. 2014. Sialic acid attenuates puromycin aminonucleoside-induced desialylation and oxidative stress in human podocytes. Exp. Cell Res 320: 258–268. [PubMed: 24200502]
35. Nan X, Carubelli I, and Stamatos NM. 2007. Sialidase expression in activated human T lymphocytes influences production of IFN-γ. J. Leukoc. Biol 81: 284–296. [PubMed: 17028199]
36. Pham ND, Pang P-C, Krishnamurthy S, Wands AM, Grassi P, Dell A, Haslam SM, and Kohler JJ. 2017. Effects of altered sialic acid biosynthesis on *N*-linked glycan branching and cell surface interactions. J. Biol. Chem 292: 9637–9651. [PubMed: 28424265]
37. Pilling D, and Gomer RH. 2018. The development of serum amyloid P as a possible therapeutic. Front. Immunol 9: 2328. [PubMed: 30459752]
38. Dillingh MR, van den Blink B, Moerland M, van Dongen MGJ, Levi M, Kleinjan A, Wijsenbeek MS, Lupher ML Jr., Harper DM, Getsy JA, et al. 2013. Recombinant human serum amyloid P in healthy volunteers and patients with pulmonary fibrosis. Pulm. Pharmacol. Ther 26: 672–676. [PubMed: 23380438]
39. Cox N, Pilling D, and Gomer RH. 2014. Serum amyloid P: a systemic regulator of the innate immune response. J. Leukoc. Biol 96: 739–743. [PubMed: 24804675]
40. Verstovsek S, Manshouri T, Pilling D, Bueso-Ramos CE, Newberry KJ, Prijic S, Knez L, Bozinovic K, Harris DM, Spaeth EL, et al. 2016. Role of neoplastic monocyte-derived fibrocytes in primary myelofibrosis. J. Exp. Med 213: 1723–1740. [PubMed: 27481130]
41. Levo Y, Wollner S, and Shalit M. 1985. Serum amyloid P-component as a marker of liver involvement in measles infection. Am. J. Gastroenterol 80: 391–392. [PubMed: 3993639]

42. Kisseleva T, Uchinami H, Feirt N, Quintana-Bustamante O, Segovia JC, Schwabe RF, and Brenner DA. 2006. Bone marrow-derived fibrocytes participate in pathogenesis of liver fibrosis. J. Hepatol 45: 429–438. [PubMed: 16846660]

43. Horgan SJ, Watson CJ, Glezeva N, Collier P, Neary R, Tea IJ, Corrigan N, Ledwidge M, McDonald K, and Baugh JA. 2015. Serum amyloid P-component prevents cardiac remodeling in hypertensive heart disease. J. Cardiovasc. Transl. Res 8: 554–566. [PubMed: 26577946]

44. Ohnishi S, Maeda S, Shimada K, and Arao T. 1986. Isolation and characterization of the complete complementary and genomic DNA sequences of human serum amyloid P component. J. Biochem 100: 849–858. [PubMed: 3029048]

45. Bucala R, Spiegel LA, Chesney J, Hogan M, and Cerami A. 1994. Circulating fibrocytes define a new leukocyte subpopulation that mediates tissue repair. Mol. Med 1: 71–81. [PubMed: 8790603]

46. Reilkoff RA, Bucala R, and Herzog EL. 2011. Fibrocytes: emerging effector cells in chronic inflammation. Nat. Rev. Immunol 11: 427–435. [PubMed: 21597472]

47. Zanchetti G, Colombi P, Manzoni M, Anastasia L, Caimi L, Borsani G, Venerando B, Tettamanti G, Preti A, Monti E, and Bresciani R. 2007. Sialidase NEU3 is a peripheral membrane protein localized on the cell surface and in endosomal structures. Biochem. J 408: 211–219. [PubMed: 17708748]

48. Pshezhetsky AV, and Ashmarina LI. 2013. Desialylation of surface receptors as a new dimension in cell signaling. Biochemistry (Mosc.) 78: 736–745. [PubMed: 24010837]

49. Miyagi T, Takahashi K, Hata K, Shiozaki K, and Yamaguchi K. 2012. Sialidase significance for cancer progression. Glycoconj. J 29: 567–577. [PubMed: 22644327]

50. Chen W, Lamb TM, and Gomer RH. 2020. TGF-γ1 increases sialidase 3 expression in human lung epithelial cells by decreasing its degradation and upregulating its translation. Exp. Lung Res 46: 75–80. [PubMed: 32102576]

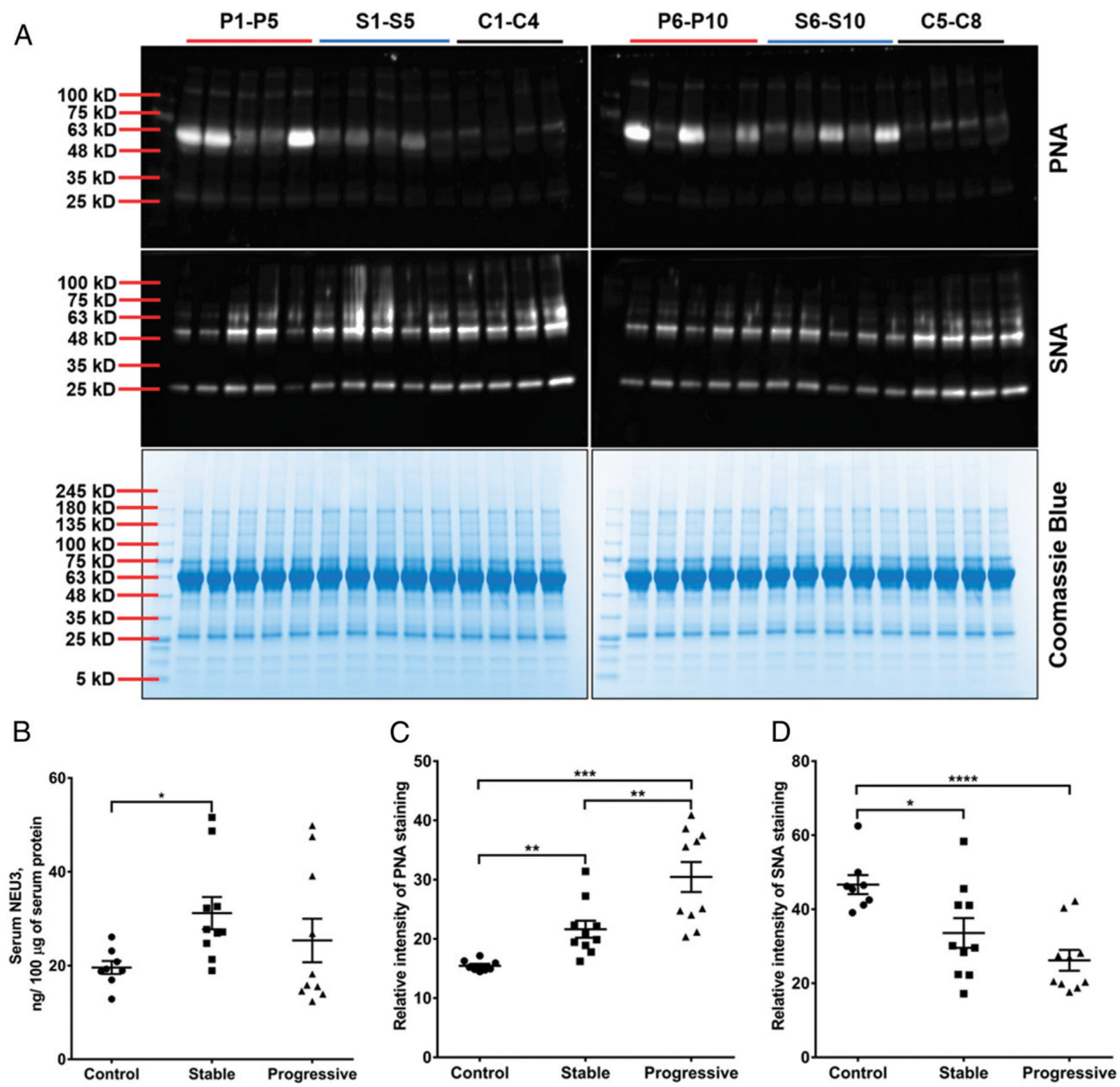

FIGURE 1. The sera of some IPF patients contains more NEU3 and more desialylated glycoprotein.

(**A**) Top, Western blots of 1:100 diluted serum samples were stained with biotinylated PNA, which binds to desialylated glycoconjugates. Middle, Western blots of 1:100 diluted serum samples were stained with biotinylated SNA, which binds to sialylated glycoconjugates. Bottom, Total serum proteins were stained with Coomassie Blue. Images are representative of three independent experiments. P1-P10 are progressive IPF, S1-S10 are stable IPF, and C1–C8 are controls. (**B**) Serum NEU3 was measured by ELISA. (**C**) The PNA-stained bands in (A) were measured by densitometry. (**D**) The SNA-stained bands in (A) were measured by densitometry. For (B)–(D), each plot symbol is the average of three independent experiments from a patient or control. Lines and error bars represent the mean ± SEM of the averages in the indicated category. *$p < 0.05$, **$p < 0.01$, ***$p < 0.001$, ****$p < 0.0001$ (one-way ANOVA, Tukey test).

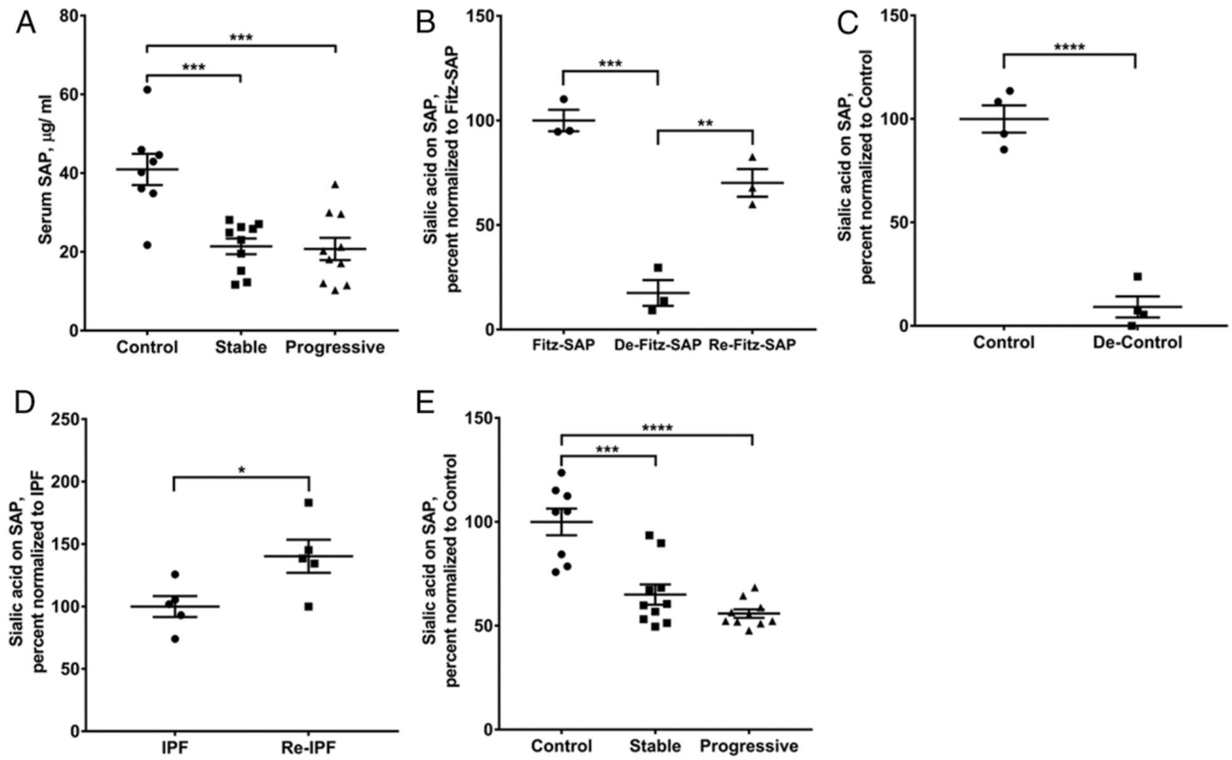

FIGURE 2. Sera from IPF patients has less SAP, and the SAP is more desialylated.

(**A**) Serum SAP was measured by ELISA. (**B**) Sialic acids on a commercial human SAP purchased from Fitzgerald Industries (Fitz-SAP) were enzymatically removed with sialidase to generate desialylated Fitz-SAP (De-Fitz-SAP). Some of the De-Fitz-SAP was resialylated with sialyltransferase to generate resialylated De-Fitz-SAP (Re-Fitz-SAP). Sialic acids on the SAPs were detected by mass spectrometry. (**C**) Sialic acids were removed from the SAP purified from four randomly selected healthy controls (De-Control). The sialic acids on the SAPs were measured by mass spectrometry. (**D**) Sialic acids were enzymatically added to the SAP purified from five randomly selected IPF patients (Re-IPF). The sialic acids on the SAPs were measured with mass spectrometry. (**E**) Sialic acids on the SAP purified from serum samples were measured by mass spectrometry. For all panels, each plot symbol is the average of three independent experiments from a patient or control. Lines and error bars represent the mean ± SEM of the averages in the indicated category. (A, B, and E), $^{**}p < 0.01$, $^{***}p < 0.001$, $^{****}p < 0.0001$ (one-way ANOVA, Tukey test). (C and D), $^{*}p < 0.05$, $^{****}p < 0.0001$ (*t* test).

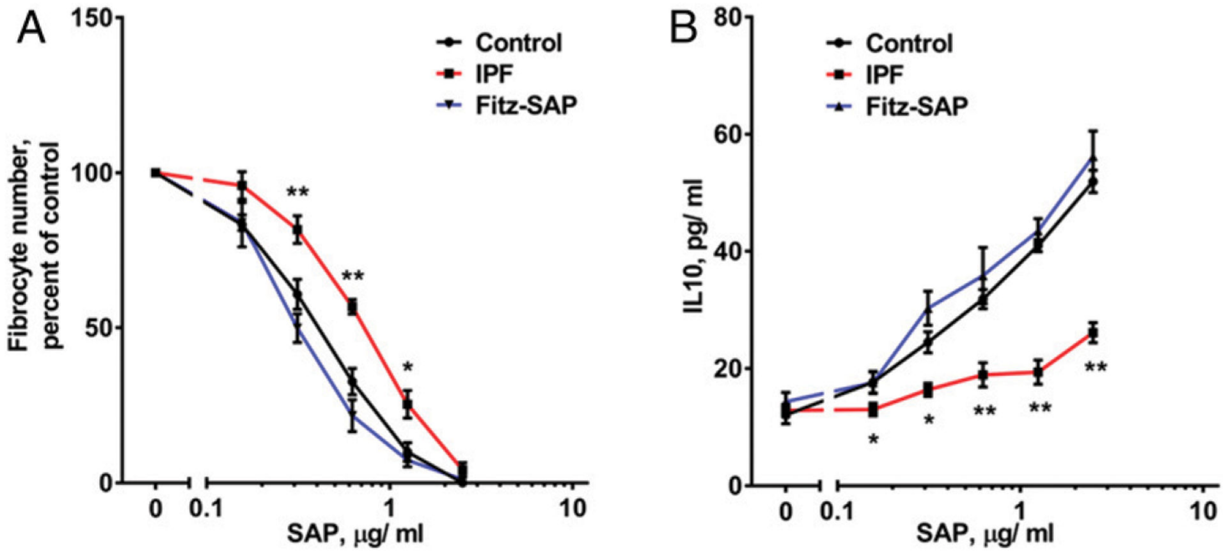

FIGURE 3. SAP from IPF patients has abnormally low bioactivities.

(**A**) The Fitz-SAP and SAP purified from serum samples were added to PBMCs for 5 d. Cells were stained with methylene blue, and fibrocytes were counted. (**B**) Culture supernatants were collected from (A) before staining. IL-10 in the supernatants was detected by ELISA. In (A) and (B), each Fitz-SAP value is the mean ± SEM of three independent assays. For control and IPF, assays were done three independent times for each serum donor, and an average was calculated for each donor. Values are mean ± SEM of the averages for the 8 controls or the 20 IPF patients. *$p < 0.05$, **$p < 0.01$, control versus IPF (*t* test).

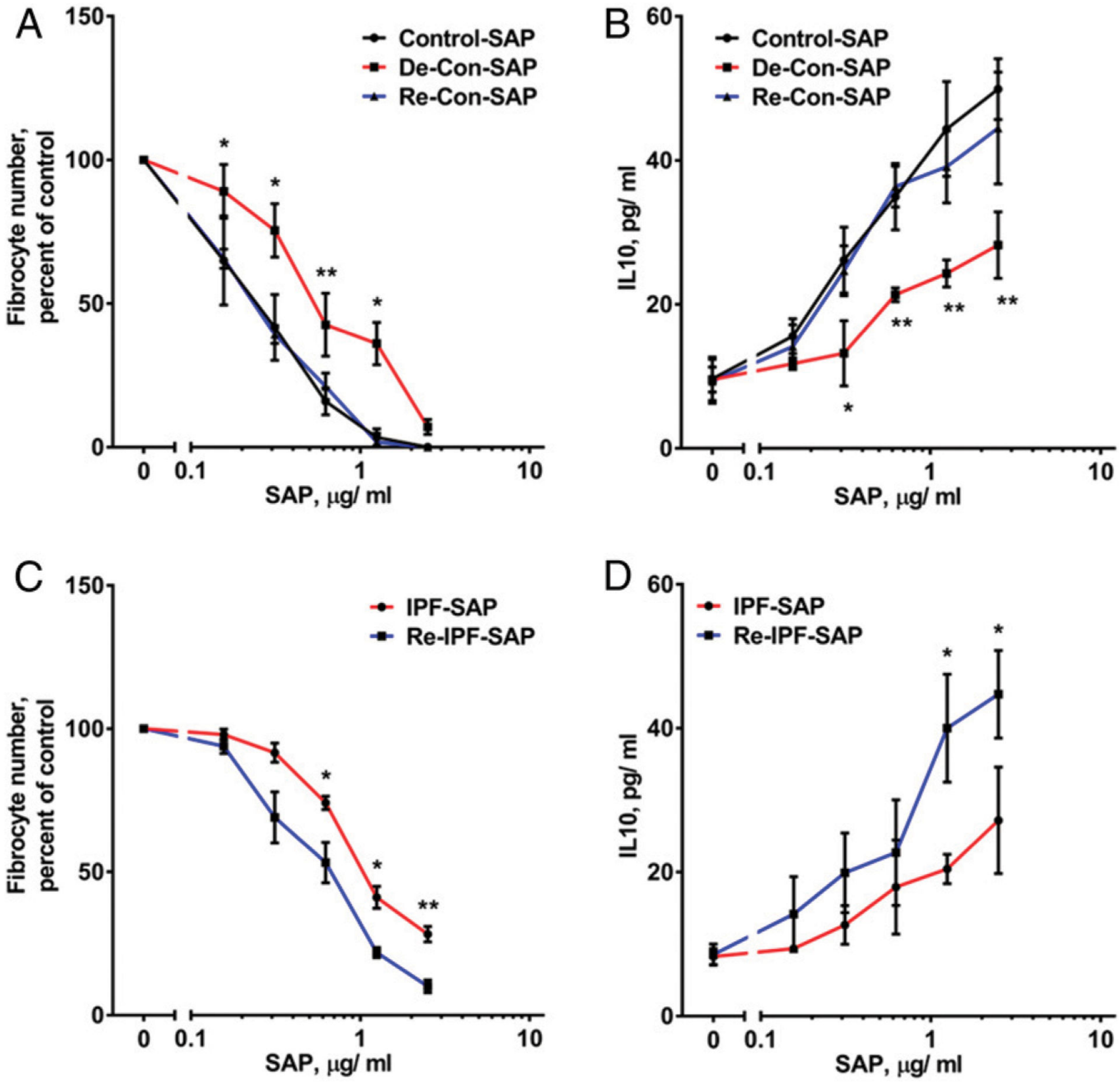

FIGURE 4. Desialylation of SAP from healthy controls and resialylation of SAP from IPF patients reverse their effects on fibrocyte differentiation and IL-10 accumulation.

(**A**) Purified SAP from four randomly selected healthy controls was enzymatically desialylated (De-Con-SAP), and some of the De-Con-SAP was then enzymatically resialylated (Re-Con-SAP). The different SAPs were added to PBMCs for 5 d. Cells were stained with methylene blue, and fibrocytes were counted. (**B**) Culture supernatants were collected from (A) before staining. IL-10 in the supernatants was detected by ELISA. For (A) and (B), assays were done three independent times for each of the four donors, and an average was calculated for each donor. Values are mean ± SEM of the four averages. *$p < 0.05$, **$p < 0.01$, control SAP versus De-Con-SAP (*t* test). (**C**) Purified SAP from five randomly selected IPF patients (IPF-SAP) was enzymatically sialylated (Re-IPF-SAP), and the SAPs were added to PBMCs for 5 d. Cells were stained with methylene blue, and fibrocytes were counted. (**D**) Culture supernatants were collected from (A) before staining.

IL-10 in the supernatants was detected by ELISA. For (C) and (D), assays were done three independent times for each of the five donors, and an average was calculated for each donor. Values are mean ± SEM of the five averages. *$p < 0.05$, **$p < 0.01$ (*t* test).

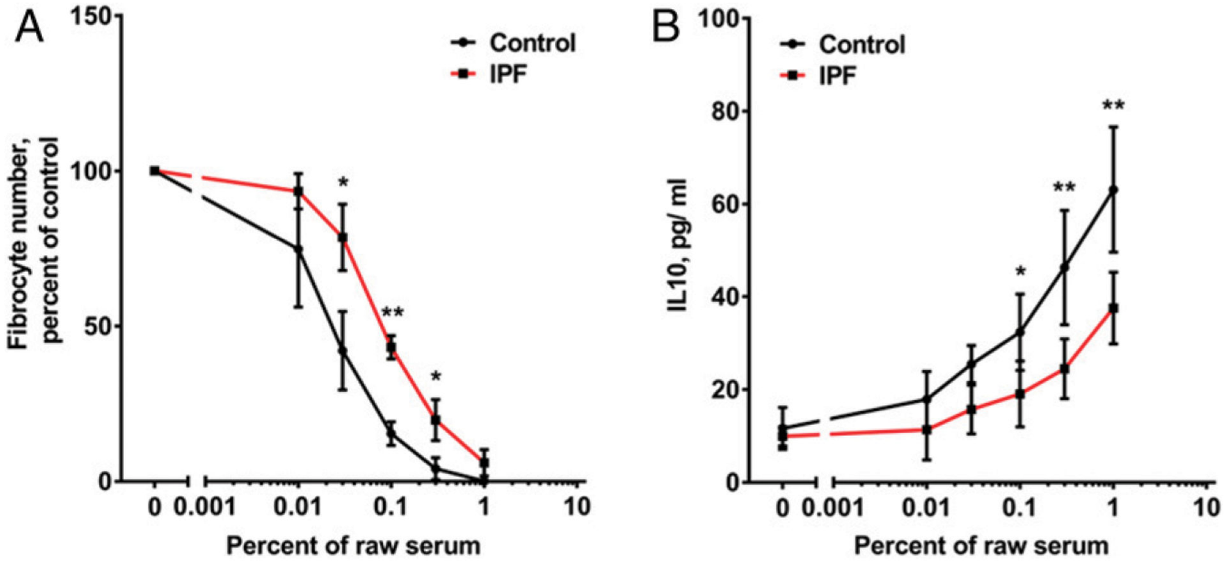

FIGURE 5. Sera from IPF patients have abnormally low bioactivity.

(**A**) Raw sera from healthy controls and IPF patients were diluted and added to PBMCs. After 5 d, cells were stained, and fibrocytes were counted. (**B**) Culture supernatants were collected from (A) before staining. IL-10 in the supernatants was detected by ELISA. In (A) and (B), assays were done three independent times for each serum donor, and an average was calculated for each donor. Values are mean ± SEM of the averages for the 8 controls or the 20 IPF patients. *$p < 0.05$, ** $p < 0.01$, control versus IPF (*t* test).

TABLE I.

Clinical details of the serum samples used in this study

	Healthy Controls	Stable IPF Patients	Progressive IPF Patients	*p* Value
n	8	10	10	
Age, y (mean ± SD)	65.6 ± 8.1	69.4 ± 5.4	72.0 ± 6.3	0.15
Gender, *n* (%)				
Male	6 (75)	8 (80)	10 (100)	0.26
Female	2 (25)	2 (20)	0 (0)	
Race, *n* (%)				
White	7 (87.5)	10 (100)	10 (100)	0.27
African American	1 (12.5)	0 (0)	0 (0)	
Smoking status, *n* (%)				
Ever	3 (37.5)	8 (80)	7 (70)	0.16
Never	5 (62.5)	2 (20)	3 (30)	
FVC% at enrollment (percentage predicted mean ± SD)		80.5 ± 13.8	71.4 ± 18.2	0.22
DLCO% at enrollment (percentage predicted mean ± SD)		52.3 ± 13.4	43.8 ± 7.8	0.10
GAP index score (mean ± SD)		3.7 ± 1.0	4.6 ± 1.6	0.14

The *p* values for age, gender, race and ethnicity, and smoking status were calculated with single-factor ANOVA or χ^2 as appropriate. The *p* values for FVC% predicted, DLCO% predicted, and GAP index were calculated with Student *t* test.